

## PREPARATION OF CONDUCTING ULTRAFILTRATION MEMBRANES FROM REDISPERSABLE, NANOSCALED, CRYSTALLINE $\text{SnO}_2\text{:Sb}$ PARTICLES.

C. GOEBBERT\*, D. BURGARD\*\*, R. NASS\*\*, M. A. AEGERTER\*, H. SCHMIDT\*\*

Institut für Neue Materialien-INM, \*Department of Coating Technology and \*\*Department of Chemistry and Technology of Nonmetallic-Inorganic Materials  
D-66123 Saarbruecken, GERMANY

Inorganic membranes prepared by the sol gel method are promising for use as filters in separation processes. Unsupported and supported conducting membranes have been produced from redispersible nanoscaled crystalline Sb-doped  $\text{SnO}_2$  powders with a Sb content up to 5 mole % (with respect to Sn). The crystalline particles are monosized ( $\cong 4$  nm) and fully redispersible in aqueous solution at  $\text{pH} \geq 8$  with a solid content up to 36.8 vol %. By thermal treatment at different temperatures and times, the pore size diameter of the material can be adjusted from 4 to 20 nm with a very narrow pore size distribution ( $\sim \pm 1$  nm) and a total porosity of 63 %, practically independent of the sintering parameters. Uniaxial compacted unsupported membranes present similar characteristics with however larger pore size distribution ( $\pm 5$  nm) and 80 % total porosity. Their electrical resistance decreases with sintering temperature and time down to  $4 \Omega$  (800 °C, 8 h). Fully dispersed aqueous solutions of the powder (7,8 vol %) were used to prepare transparent conducting porous coatings on glass or ceramics by spin-coating. After thermal treatment (1 hour at 550 °C) single layers 200 nm thick have a typical specific electrical resistance  $\rho = 2.5 \cdot 10^{-2} \Omega\text{cm}$  and an optical transmission in the visible range measured against air of 90 %.

### 1. INTRODUCTION

There is a growing interest for microbiological resistant and chemically stable materials in the development of membranes for separation processes. Polymeric materials deteriorate above 200 °C or in the presence of organic solvents and do not always have the desired porous texture. Ceramic materials (such as alumina, silica, titania, zirconia, etc.) fulfil these requirements and are presently used in the preparation of membranes for microfiltration, ultrafiltration and hyperfiltration with pore sizes ranging between 100 to 1000 nm, 2 to 100 nm and  $< 2$  nm respectively<sup>1</sup>. The sol-gel process is a versatile technique for the preparation of ceramic membranes as it allows the control of the pore size and pore distribution<sup>2</sup>. The major problem lies in the obtention of thick coatings ( $> 1 \mu\text{m}$ ) which may crack during the postsynthesis drying and sintering stages. Sol-gel research in the field of micro- and ultrafiltration membranes has involved  $\text{Al}_2\text{O}_3$ ,  $(\text{SiO}_2)^{3-7}$ , transition metal oxides such as  $\text{TiO}_2$ ,  $\text{ZrO}_2^{7-9}$  and  $\text{SnO}_2^{10-12}$ .

A novel and promising process for the obtention of oxide membranes for ultrafiltration and coatings using of redispersable, nanoscaled crystalline powder<sup>13</sup> is presented. The paper describes the preparation and characterisation of such powders, of unsupported and supported conducting membranes and of conducting coatings made by the spin coated process<sup>14</sup>. The combination of conductivity or photocatalytic properties may be an asset for the development of membranes for hybrid processes.

## 2. EXPERIMENTAL PROCEDURE

### 2.1. Powder and membrane preparation

SnO<sub>2</sub> and SnO<sub>2</sub>:Sb particles were prepared by a controlled growth technique<sup>14-17</sup>. A solution of tin(IV) chloride in ethanol containing up to 10 mole % of SbCl<sub>3</sub> was added dropwise to an aqueous ammonia solution containing 10 wt. %, with respect to the oxide, of a surface modifying agent,  $\beta$ -alanine. The prepared suspensions were then treated in an autoclave at 150 °C and 10 bar for 3 hours. The resulting powder was isolated by centrifugation, washed with water several times and then dried at 60 °C. Such a powder is fully redispersable in water at pH  $\geq$  8 under ultrasonic irradiation. The size of the particles was measured by High Resolution Transmission Microscopy (HRTEM). The analysis of the pore characteristics was performed by BET measurement (ASAP2400, Micromeritics) on loose powder and uniaxial compacted membranes thermally treated at different temperatures (400 to 800 °C) and times (10, 30, 90, 300 min). The materials were also characterised by X-ray diffraction (XRD) and density measurement with a pycnometer (AccuPyc1330, Micromeritics).

### 2.2. Coating preparation

Colloidal suspensions were prepared by dispersing the non-thermally treated powder in water at pH  $\geq$  11 using 0.78 mole/l tetramethylammoniahydroxide (TMAH) as a base. After powder addition the resulting suspensions were submitted to ultrasound irradiation for 2 minutes. After this treatment the suspensions were stirred for one day. The final dispersions were clear with a yellowish orange colour. Stable suspensions can be obtained up to a solid content of 36,8 vol %.

Crackfree conducting coatings on borofloat glass or alumina substrates have been prepared using the spin coating process (2500 rpm, 15 s) using solution with a solid content up to 7,7 vol %. The thermal densification of the film was carried out at temperatures from 400 to 600 °C for 0.25 to 8 h. The film thickness was measured with a Tencor P10 surface profiler. The characterisation of the electrical properties was carried out by the 4-point and van der Pauw/Hall

technique (MMR Technologies). The pore size distribution has been measured by surface acoustic wave (SAW) technique.

### 3. RESULTS AND DISCUSSION

#### 3.1. Powder characterisation

The structure of the dried  $\text{SnO}_2$  and  $\text{SnO}_2\text{:Sb}$  powders is shown in Figure 1. The particles are already crystalline and have a cassiterite structure.

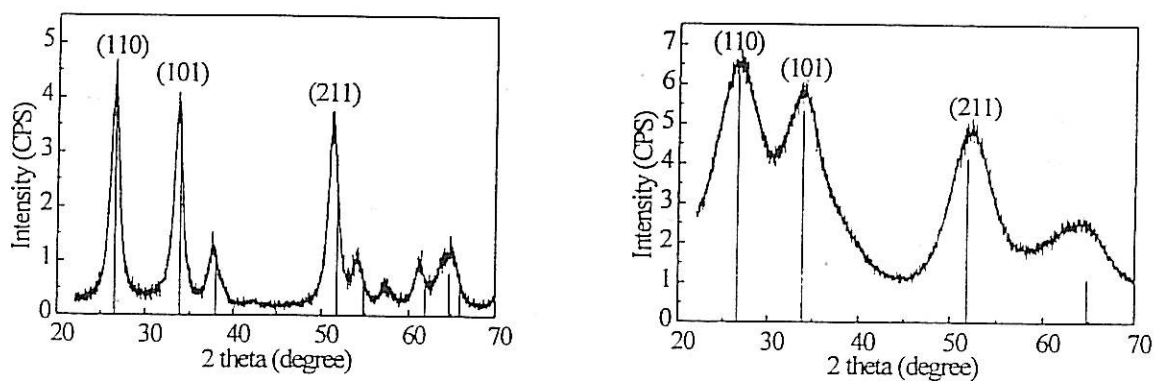


Figure 1

X-ray diffraction spectra of dried powder. Left:  $\text{SnO}_2$ , right:  $\text{SnO}_2\text{:Sb}$  (5 mole %)

The vertical lines drawn on the figure correspond to the data taken from the JCPDS for this structure. The particles are not oriented and the crystallite size, calculated with a Siemens software for the (110) peak, is 7 nm for  $\text{SnO}_2$  and 3 nm for  $\text{SnO}_2\text{:Sb}$ . A systematic decrease was observed with increasing antimony content.

The size of the particle was confirmed by HRTEM measurements. Figure 2 shows a picture of a dried droplet of a suspension showing crystalline particles with an average size of 3 to 5 nm with no evidence of aggregation. Each particle is probably formed by a single crystallite.

The evolution of the porosity of the powder and uniaxial compacted membranes after different heat treatment is practically identical. Figure 3 shows as an example the  $\text{N}_2$  adsorption and desorption isotherms of the compacted membranes. The BET isotherms have a type IV shape at all temperatures<sup>19</sup>. The hysteresis is of type  $H_2$  at low temperature and is typical for capillary condensation inside ink-bottle shaped mesopores of corpuscular systems. At high sintering temperatures the hysteresis tends towards a  $H1$  type indicating a higher regularity of the cross

section along the longitudinal direction of the pores (transformation of an ink-bottle shape towards a cylindrical shape<sup>10</sup>).

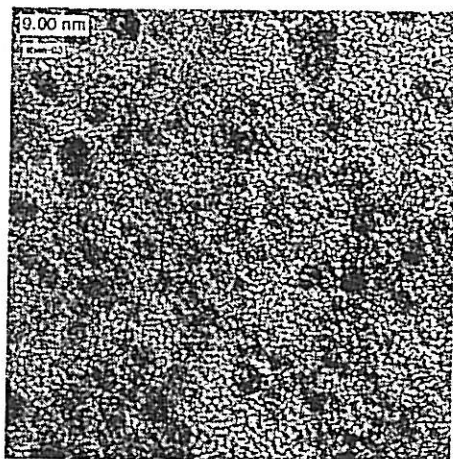


Figure 2

HRTEM picture of nanocrystalline  $\text{SnO}_2\text{:Sb}$  powder redispersed in water and TMAH.

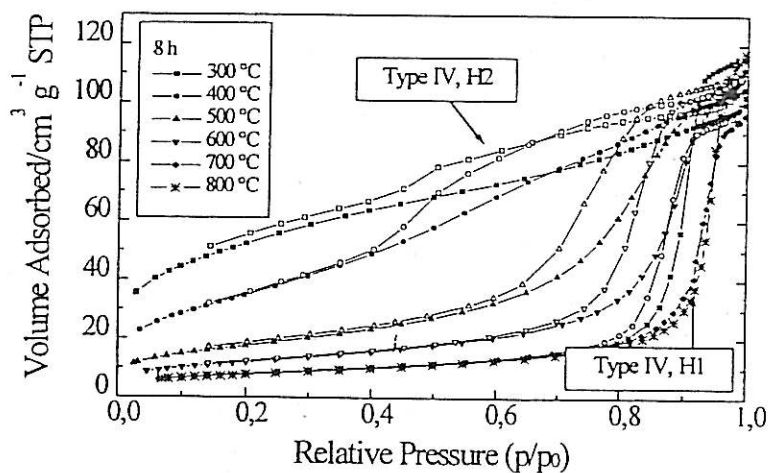


Figure 3

$\text{N}_2$  adsorption and desorption isotherms of uniaxial compacted  $\text{SnO}_2\text{:Sb}$  membranes heat treated at different temperatures during 5 h. (solid symbol = adsorption; open symbol = desorption)

The pore size distribution curves were determined from the desorption branches. Figure 4 indicates a gradual increase of the pore size with the temperature of the heat treatment. For 400 °C, 10 min or lower temperature the pore size distribution is large showing the presence of micropores. By increasing the sintering temperature, the pore size distribution become narrower, about  $\pm 5$  nm, and the average diameter shifts from 4 nm (400 °C) to 20 nm (800 °C) while the maximum pore volume increases steadily to a value of about 0.8  $\text{cm}^3/\text{g}$ . A longer sintering time gives a better defined pore size distribution with a slight shift of their size. There are some

interesting differences between the results obtained for undoped  $\text{SnO}_2$  xerogel<sup>10</sup> and ours. For  $\text{SnO}_2:\text{Sb}$  prepared by a controlled growth reaction, the pore volume is always higher than that of  $\text{SnO}_2$  xerogel especially for the distribution at 400 °C and for those at  $T \geq 700$  °C. At 700 °C the maximum pore volume of undoped  $\text{SnO}_2$  xerogel is already strongly reduced and at 800 °C is not measurable, while for  $\text{SnO}_2:\text{Sb}$  the volume is still high  $\sim 0,8 \text{ cm}^3/\text{g}$ .  $\text{SnO}_2:\text{Sb}$  is therefore better indicated for the realisation of membranes, where the pore diameter can be continuously adjusted with the sintering temperature and time with a narrow distribution in the range of 4 to 20 nm. The total porosity of the membranes is 80 %, practically independent of the sintering conditions.

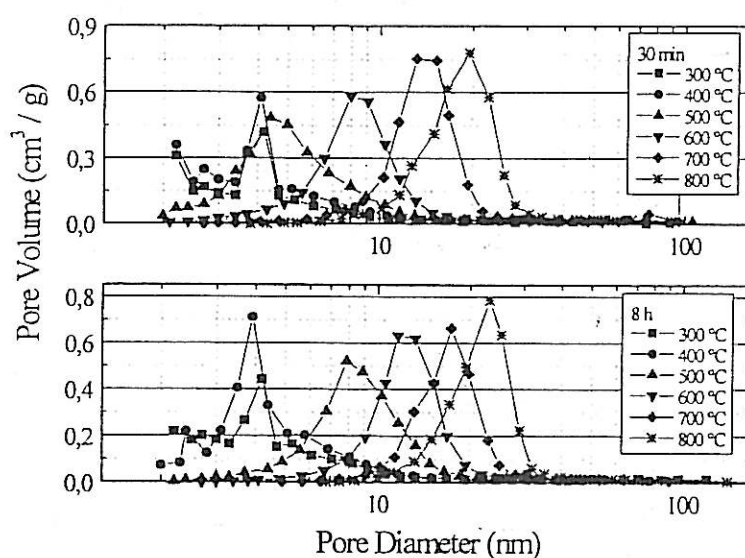


Figure 4

Evolution of pore characteristics (volume, size) of uniaxial compacted membranes with sintering temperature and time.

With the increase of the temperature and the sintering time the surface area decreases and reaches a minimum for each temperature for sintering time longer than about 8 hours. At higher temperature the reduction of the BET surface with the sintering time is smaller and in agreement with the change of the isotherm from type IV-H2 to type IV-H1 (better regularity). The true density increases in parallel with the sintering temperature and time and reaches at 800 °C values of the theoretical density (figure 5). The overall behaviour is in agreement with the results found by Santilli et al<sup>20</sup> for  $\text{SnO}_2$  xerogel, indicating that the sintering behaviour of  $\text{SnO}_2:\text{Sb}$  obey a dynamic scaling model as for  $\text{SnO}_2$  and that this material can be seen as a two phases system composed by a nearly homogeneous  $\text{SnO}_2:\text{Sb}$  matrix with high concentration of vacancy and empty microvoid. The total volume fraction of both phases (80 % for the porous phase, 20 % for the solid phase) remains constant at least up to 800 °C and the solid fraction reaches the

theoretical value of the density at high temperatures (800 °C). Under these conditions no significant bulk densification occurs in this temperature range, confirming the great interest of this material for the realisation of ultrafiltration membranes. Dried membranes have a high electrical resistance. The value drastically decreases with sintering temperature and time from 360 K $\Omega$  (300 °C, 30 min) down to 4  $\Omega$  for T>700 °C. These values are higher than those obtained with coatings (see below).

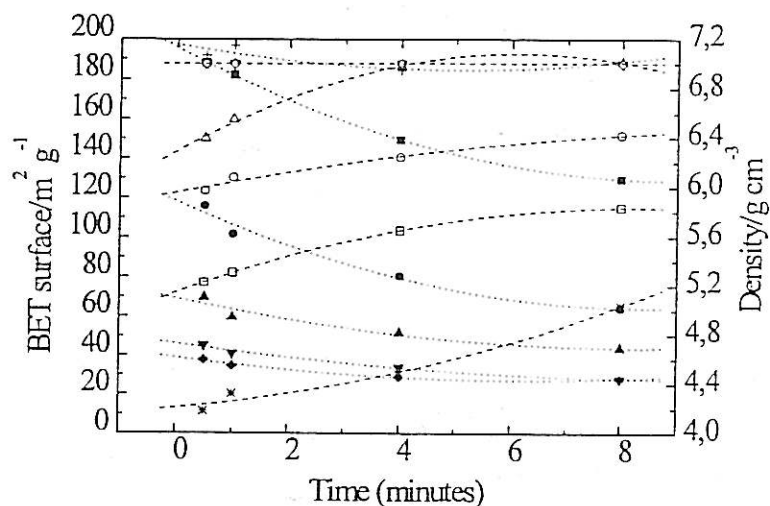


Figure 5

Influence of temperature and sintering time on the BET surface area and the true density of SnO<sub>2</sub>:Sb pellets. (●/○ 400 °C, ■/□ 500 °C, ▲/△ 600 °C, ▼/▽ 700 °C, ◆/◇ 800 °C, solid symbol = BET surface area; open symbol = density)

### 3.2. Film characterisation

Films have been deposited on glass and alumina substrates using the spin coating technique. Each film was densified in a furnace immediately after the spin coating process. After firing, the films are uniform with a roughness, measured by AFM, as small as  $R < 3$  nm. Thickness as high as 500 nm can be obtained for a single layer. Thicker coatings (up to 1.5  $\mu$ m) have been prepared by repeating the coating and sintering processes.

The lowest resistivities are reached with a 7,7 vol % solid content of the solution. With higher concentration the films start to crack. With this concentration single layers have a thickness of 200 nm after firing. As for the compacted substrate, the electrical resistance of the films decreases with the temperature and time of the sintering process (figure 6) down to  $\rho = 2.5 \cdot 10^{-2}$   $\Omega$ cm, (550 °C, 1 h). Such coatings have an electron mobility  $\mu = 1$  cm<sup>2</sup>/Vs and an electron density  $n = 2,15 \cdot 10^{20}$  cm<sup>-3</sup>. The optical transmission in the visible range is 85-90 %.

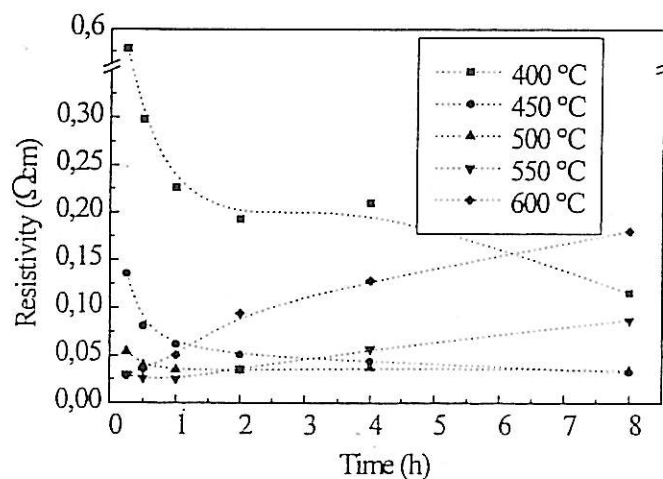


Figure 6

Resistivity vs sintering time for different sintering temperatures. Films were made with a 7,7 vol % particle concentration in the sol.

HRTEM cross-sections of multi-layer films show that they are made of porous and interconnected particles, a denser layer (~20 nm thick) being observed on top of each layer. This layer has a higher conductivity than the bulk of the coating<sup>21</sup>. However, if each layer is dried at 150 °C between each deposition and the multilayer coating sintered as a whole at higher temperature, these denser layers do not occur and the morphology of the whole coating is homogeneous. The resistivity of the coatings is smaller than that of the compacted membranes. The pore size distribution of 140 nm thick coating has been evaluated by SAW technique at 300 °C. The average diameter values (4,5 nm) are similar to that shown in figure 4 with values at half maximum of 3,5 and 8 nm. Assuming a coating density<sup>21</sup> of 4,0 g/cm<sup>3</sup> the BET surface area is 80 m<sup>2</sup>/g (~ 45 cm<sup>2</sup> per cm<sup>2</sup> of geometrical coating area), a value much smaller than that of the powder (178 m<sup>2</sup>/g).

#### 4. CONCLUSION

Nanoscaled, crystalline SnO<sub>2</sub> and SnO<sub>2</sub>:Sb particles fully redispersable in water have been prepared. The growth of the particles in a solution was controlled by chemical modification of the particle surface using β-alanine. Dried powders can be fully redispersed in water. Suspension with solid content up to 36,8 vol % are stable for pH > 8. Thick coating (up to 0.5 μm/layer) have been obtained by spin coating process. The specific resistivity of SnO<sub>2</sub>:Sb coatings depends on the thickness, the particle concentration, temperature and time of the sintering process. Resistivity values as low as  $\rho = 2,5 \cdot 10^{-2} \Omega\text{cm}$  and sheet resistance as low as  $R_{\square} = 60 \Omega_{\square}$  has been obtained for a 7- layer coating (thickness 1,4 μm). Uniaxial compacted membranes heat treated in air

exhibit microporosity with narrow pore size distribution ( $\pm 5$  nm). The pore size can be continuously varied in a controlled way between 4 nm (400°C) to 20 nm (800°C). These materials offer high chemical and thermal resistance and is therefore promising for industrial preparation of conducting membranes for ultrafiltration and transparent conducting layer for antistatic application or for systems which need sheet resistance larger than about  $100 \Omega_{\square}$  such as touch screen panels.

#### ACKNOWLEDGEMENT

Research supported by BMBF (2 A 67/03 N 9040) and the state of Saarland (Germany)

#### REFERENCES

- 1) R. R. Bhave, *Inorganic Membranes: Synthesis, Characteristics and Application*, Van Nostrand Reinhold, New York 1991.
- 2) C. J. Brinker, G. W. Scherer, *Sol-Gel Science: The physics and chemistry of sol-gel processing*, Acad. Press Inc., San Diego, USA 1990.
- 3) A. F. M. Leenaars, K. Keizer, A. J. Burggraaf, *J. Mat. Sci.* **19** (1984), 1077.
- 4) A. Larbot, S. Alami-Younssi, M. Persin, J. Sarrazin, L. Cot, *J. Membr. Sci.* **97** (1994), 167.
- 5) M. I. D. d. Albani, C. P. Arciprete, *J. Membr. Sci.* **69** (1992), 21.
- 6) C. J. Brinker, N. K. Raman, M. N. Logan, R. Sehgal, R. A. Assink, D. W. Hua, T. L. Ward, *J. Sol-Gel Sci. Tech.* **4** (1995), 117.
- 7) L. C. Klein, C. Yu, R. Woodman, R. PAvlik, *Catal. Today* **14** (1992), 165.
- 8) A. Larbot, J. P. Fabre, L. Cot, *J. Amer. Ceram. Soc.* **72** (1989), 257.
- 9) C. Guizard, A. Julbe, A. Larbot, L. Cot, *J. Alloys Comp.* **8** (1992), 188.
- 10) G. E. S. Brito, S. H. Pulcinelli, C. V. Santilli, *J. Sol-Gel Sci. Tech.* **2** (1994), 575.
- 11) L. R. B. Santos, S. H. Pulcinelli, C. V. Santilli, *J. Sol-Gel Sci. Tech.* **8** (1997), .
- 12) L. R. B. Santos, S. H. Pulcinelli, C. V. Santilli, *J. Memb. Sci.* **127** (1997), 77-86.
- 13) D. Burgard, C. Goebbert, R. Nass, *J. Sol-Gel Sci. Tech.* (in press) .
- 14) C. Goebbert, M. A. Aegerter, D. Burgard, R. Nass, H. Schmidt, in "Chemical and Pyrolytic Routes to Nanostructured Powders and Their Industrial Application, MRS 520 (in press)
- 15) D. Burgard, R. Nass, H. Schmidt, in *Aqueous Chemistry and Geochemistry of Oxides, Oxyhydroxides and related Materials*, MRS 432, pp. 113-20 (1997).
- 16) D. Burgard, R. Nass, H. Schmidt, *Werkstoffwoche, Symp. 6 Werkstoff und Verfahrenstechnik*, pp. 569-77 (1997).
- 17) D. Burgard, C. Kropf, R. Nass, H. Schmidt, in *Better Ceramics through Chemistry*, MRS 346 pp. 101-7 (1994).
- 18) J. Persello, A. Magnin, J. Chang, J. M. Piau, B. Cabane, *J. Rheol.* **38** (1994), 1845.
- 19) IUPAC, *Pure Appl. Chem.* **57** (1985), 603.
- 20) C. V. Santilli, S. H. Pulcinelli, D. F. Craierich, *Phys. Rev. B* **51** (1995), 8801-9.
- 21) J. Pütz, D. Ganz, G. Gasparro, M. A. Aegerter, *J. Sol-Gel Sci. Tech.* (in press)



ADVANCES IN SCIENCE AND TECHNOLOGY, 16

# CERAMICS: GETTING INTO THE 2000's

Proceedings of the World Ceramics Congress, part of the  
9th CIMTEC-World Ceramics Congress and Forum on New Materials  
Florence, Italy June 14-19, 1998

PART D Including:

Section I - *Structural Ceramics*

Section J - *Ceramics for Process Engineering, Chemical and  
Environmental Applications*

Section SM - *Standards and Markets for ATCs*

Edited by

P. VINCENZINI

*National Research Council, Italy*

TECHNA

Faenza 1999